A SINGLE-PHASE ACTIVE DEVICE FOR QUALITY IMPROVEMENT OF ELECTRIFIED TRANSPORTATION

V.Manasa¹, Dr.N.V Subbarao²

¹M.Tech Student, Anu Bose Institute of Technology, Paloncha, khammam, Telangana, India

²Prof Dept of EEE, Anu Bose Institute of Technology, Paloncha, khammam, Telangana, India

ABSTRACT:

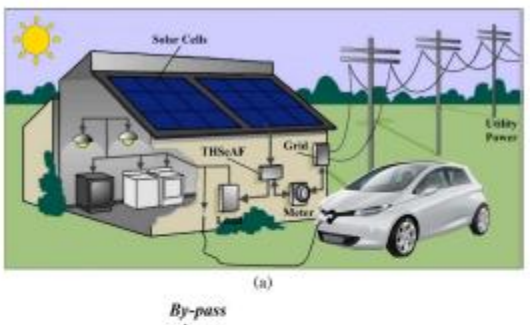
Transformer less hybrid series active filteris proposed to enhance the power quality in singlephase systems with critical loads. This paper assists the energy management and power quality issues related to electrictransportation and focuses on improving electric vehicle load connection to the grid. The control strategy is designed to prevent current harmonic distortions of nonlinear loads to flow into the utility and corrects the power factor of this later. While protecting sensitive loads from voltage disturbances, sags, and swells initiated by the power system, ridded of the series transformer, the configuration is advantageous for an industrial implementation. This polyvalent hybrid topology allowing the harmonic isolation and compensation of voltage distortions could absorb or inject the auxiliary power to the grid. Aside from practical analysis, this paper also investigates on the influence of gains and delays in the real-time controller stability. The simulations and experimental results presented in this paper were carried out on a 2-kVA laboratory prototype demonstrating the effectiveness of the proposed topology.

Index Terms—Current harmonics, electric vehicle, hybrid series active filter (HSeAF), power quality, real-time control.

INTRODUCTION:

THE forecast of future Smart Grids associated with electric vehicle charging stations has created a serious concern on all aspects of power quality of the power system, while widespread electric vehicle battery charging units [1], [2] hav detrimental effects on power distribution system harmonic voltage levels [3]. On the other hand, the growth o harmonics fed from nonlinear loads like electric vehicle propulsion battery chargers [4], [5], which indeed have detrimental impacts on the power system and affect plant equipment, should be considered the increased rms and peak value of the distorted current waveforms increaseheating and losses and cause the failure of the electrical equip Moreover, to protect the point of common coupling (PCC) voltage restorer(DVR) function is advised. A solution is to reduce the pollution of power electronics-based loads directly at their source. Although several attempts are made for a specific case study, a generic solution is to be explored. There exist two types of active power devices to overcome the described power quality issues. The first category are series active filters (SeAFs), including hybridtype ones. They were developed to eliminate current harmonics produced by nonlinear load from the power system. SeAFs are less scattered than the shunt type of active filters [8], [9]. The advantage of the SeAF compared to the shunt type is the inferior rating of the compensator versus the load nominal rating [10]. However, the complexity of the configuration and necessity of an isolation series transformer had decelerated their industrial application in the distribution concern of addressing voltage issues on sensitive loads. Commonly known as DVR, they have a similar configuration as the SeAF. These two categories are different from each other in their control principle. This difference relies on the purpose of the irapplication in the system

International Journal of Engineering In Advanced Research Science and Technology ISSN: 2278-2566



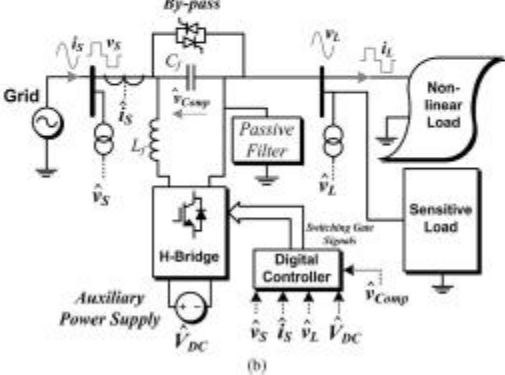


Fig. 1. (a) Schematic of a single-phase smart load with the compensator installation. (b) Electrical diagram of the THSeAF in a single-phase utility.

isolation transformer and promotes industrial application for filtering purposes. The setup has shown great ability to perform requested compensating tasks for the correction of current and voltage distortions, PF correction, and voltage restoration on This paper is organized as follows. The system architecture is introduced in the following section. Then, the operation

principle of the proposed configuration is explained. The third section is dedicated to the modeling and analysis of the control algorithm implemented in this work. The dc voltage regulationand its considerations are briefly explained, and the voltage and current harmonic detection method is explicitly described. To evaluate the configuration and the control approach, some scenarios are simulated. Experimental results performed in the laboratory are demonstrated to validate simulations. This paper is summarized with a conclusion and appendix where further mathematical developments are demonstrated.

II. SYSTEM ARCHITECTURE:

The THSeAF shown in Fig. 1 is composed of an H-bridge converter connected in series between the source and the load. A shunt passive capacitor ensures a low impedance path for current harmonics. A dc

auxiliary source could be connected to inject power during voltage sags. The dc-link energy storage

TABLE I CONFIGURATION PARAMETERS

Symbol	Definition	Value
v_s	Line phase-to-neutral voltage	120 Vrms
f	System frequency	60 Hz
Raon-linear load	Load resistance	11.5 Ω
Lnon-linear load	Lond inductance	20 mH
P_L	Linear load power	1 kVA
PF	Linear load power factor	46 %
Lf	Switching ripple filter inductance	5 mH
Cf	Switching ripple filter capacitance	2 μF
T_S	dSPACE Synchronous sampling time	40 μs
f _{РИМ}	PWM frequency	5 kHz
G	Control gain for current harmonics	8 Ω
V_{DCref}^*	VSI DC bus voltage of the THSeAF	70 V
PI_G	Proportional gain (K_p) , Integral gain (K_l)	0.025(4*), 10 (10*)

^{*} Adopted value for the experimental setup

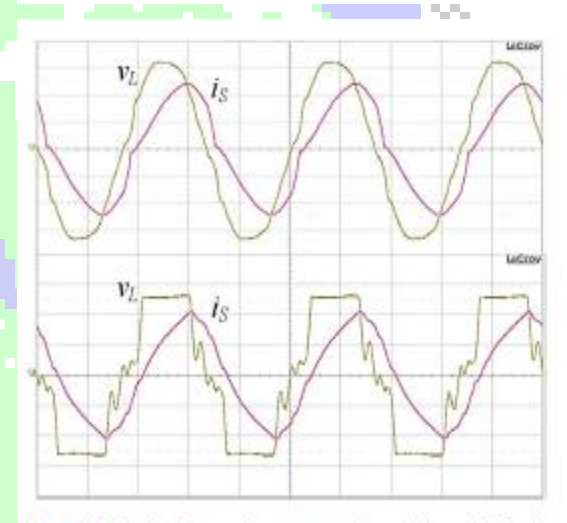


Fig. 2. Terminal voltage and current waveforms of the 2-kVA singlephase system without compensator. (a) Regular operation. (b) Grid's voltage distortion (scales: 50 V/div for channel 1 and 10 A/div for channel 2).

system is described in [19]. The system is implemented for a rated power of 2200 VA. To ensure a fast transient response with operation, the controller is implemented on a dSPACE/dsp1103. The system parameters are identified in Table I. A variable source of 120 Vrms is connected to a 1.1-kVA nonlinear load and a 998-VA linear load with a 0.46 PF. The THSeAF is connected in series in order to inject the compensating voltage. On the dc side of the compensator, an auxiliary dc-link energy storage system is installed. Similar parameters are also applied for practical implementation.

TABLE II Single-Phase Comparison of the THSeAF to Prior HSeAFs

Definition	Proposed THSeAF	[21]	[22]	[12]
Injection Transformer	Non	2 per phase	1 per phase	1 per phase
# of semiconductor devices	4	8	4	4
# of DC link storage elements	1+Aux. Pow.	1	2	1+Aux. Pow.
AF rating to the load power	10-30%	10-30%	10-30%	10- 30%
Size and weight, regarding the transformer, power switches, drive circuit, heat sinks, etc.	The Lowest	High	Good	Good
Industrial production costs	The Lowest	High	Low	Low
Power losses, including switching, conducting, and fixed losses	Low	Better	Low	Low
Reliability regarding independent operation capability	Good	Low	Good	Good
Harmonic correction of Current source load	Good	Good	Good	Low
Voltage Harmonic correction at load terminals	Good	Better	Good	Good
Power factor correction	Yes	Yes	Yes	No
Power injection to the grid	Yes	No	No	Yes

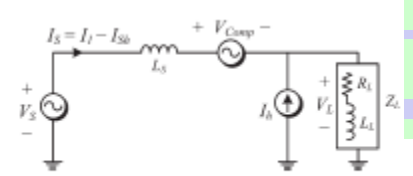


Fig. 3. THSeAF equivalent circuit for current harmonics.

perform

the compensation of current issues and maintaining a constant voltage free of distortions at the load terminals. The behavior of the SeAF for a current control approach is evaluated from the phasor's equivalent circuit shown in Fig. 3. The nonlinear load could be modeled by a resistance representing the active power consumed and a current source generating current harmonics. Accordingly, the impedance ZL represents the nonlinear load and the inductive load. The SeAF operates as an ideal controlled voltage source (V comp) having a gain (G) proportional to the current harmonics (Ish) flowing to the grid (Vs)

frequency creates a low-impedance path for all harmonics and open circuit for the fundamental; it also helps

for PF correction.

$$V_{\text{comp}} = GI_{sh} - V_{Lh}. \qquad (1)$$

This allows having individual equivalent circuit for the funmental and harmonics

$$V_{\text{source}} = V_{s1} + V_{sh}, \quad V_L = V_{L1} + V_{Lh}.$$
 (2)

The source harmonic current could be evaluated

Combining (3) and (4) leads to (5)

$$V_{sh} = -Z_s I_{sh} + V_{comp} + V_{Lh}$$
(3)

 $V_{Lh} = Z_L(I_h - I_{sh}).$

$$I_{sh} = \frac{V_{sh}}{(G - Z_s)}.$$
 (5)

gain G is sufficiently large $(G \rightarrow \infty)$, the source current will become clean of any harmonics $(Ish \rightarrow 0)$. This will

help improve the voltage distortion at the grid side. In this approach, the THSeAF behaves as high-impedance open circuit for current harmonics, while the shunt high-pass filter tuned at the system III. MODELING AND CONTROL OF THE

SINGLE-PHASE THSeAF:
Based on the average equivalent circuit of an inverter
[23], the small-signal model of the proposed
configuration can be

obtained as in Fig. 4. Hereafter, d is the duty cycle of the upper switch during a switching period, whereas $\overline{}v$ and $\overline{}i$ denote the average values in a switching period of the voltage and current

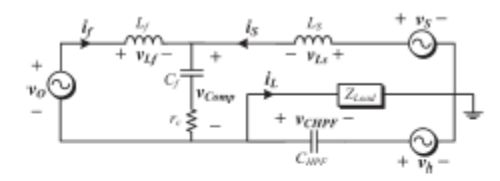


Fig. 4. Small-signal model of transformerless HSeAF in series between the grid and the load.

of the same leg. The mean converter output voltage and current are expressed by (6) and (7) as follows:

$$\bar{v}_O = (2d - 1)V_{DC}$$
 (6)

where the (2d-1) equals to m, then

$$\bar{i}_{DC} = m\bar{i}_f$$
. (7)

· If the harmonic frequency is high enough, it is possible assume that there will be no voltage harmonics across the load. The state-space small-signal ac model could be derived by linearized perturbation of the averaged model as follows:

Hence, we obtain
$$\frac{d}{dt}\begin{bmatrix} \frac{v_{Cf}}{v_{CHPF}} \\ \frac{\bar{i}_S}{\bar{i}_f} \\ \frac{\bar{i}_f}{\bar{i}_L} \end{bmatrix} = \begin{bmatrix} 0 & 0 & \frac{1}{C_f} & \frac{1}{C_f} & 0 \\ 0 & 0 & \frac{1}{C_{HPF}} & 0 & -1/C_{HPF} \\ 0 & 0 & \frac{1}{C_{HPF}} & 0 & -1/C_{HPF} \\ -1/L_S & -1/L_S & -r_c/L_S & -r_c/L_S & 0 \\ -1/L_f & 0 & -r_c/L_f & -r_c/L_f & 0 \\ 0 & \frac{1}{L_L} & 0 & 0 & -R_L/L_L \end{bmatrix} \\ \times \begin{bmatrix} v_{Cf} \\ \bar{v}_{CHPF} \\ \bar{\iota}_S \\ \bar{\iota}_f \\ \bar{\iota}_L \end{bmatrix} + \begin{bmatrix} 0 & 0 & 0 \\ 0 & 0 & 0 \\ \frac{1}{L_S} & 0 & \frac{1}{L_S} \\ 0 & \frac{1}{L_S} & 0 \end{bmatrix} \times \begin{bmatrix} v_S \\ V_{DC} \\ v_h \end{bmatrix}. \quad (10)$$

Moreover, the output vector is

$$y = Cx + Du$$
 (11)

$$\begin{bmatrix} \bar{v}_{\text{comp}} \\ \bar{v}_L \end{bmatrix} = \begin{bmatrix} 1 & 0 & r_c & r_c & 0 \\ 0 & 1 & 0 & 0 & 0 \end{bmatrix} \times \begin{bmatrix} \bar{v}_{Cf} \\ \bar{v}_{CHPF} \\ \bar{i}_S \\ \bar{i}_f \\ \bar{i}_L \end{bmatrix}$$

$$+ \begin{bmatrix} 0 & 0 & 0 \\ 0 & 0 & -1 \end{bmatrix} \times \begin{bmatrix} \bar{v}_S \\ V_{DC} \\ \bar{v}_h \end{bmatrix}. \quad (12)$$

By means of (10) and (12), the state-space representation of the model is obtained as shown in Fig. 4. The transfer function of the compensating voltage versus the load voltage, $TV_CL(s)$, and the source current, TCI (s), are developed in the Appendix. Meanwhile, to control the active

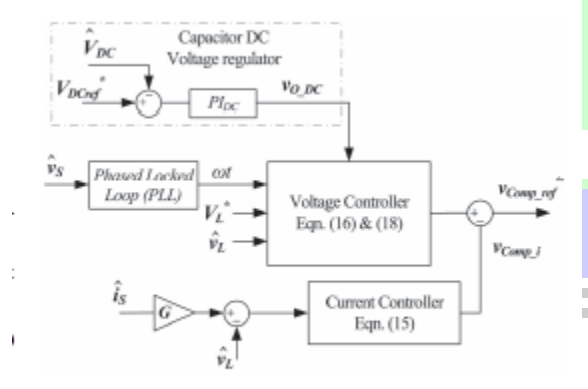


Fig. 5. Control system scheme of the active part.

dc auxiliary source should be employed to maintain an adequate supply on the load terminals. During the sag or swell conditions, it should absorb or inject power to keep the voltage magnitude at the load terminals within a specified margin. However, if the compensation of sags and swells is less imperative, a capacitor could be deployed. Consequently, the dclink voltage across the capacitor should be regulated as demonstrated

IV. SIMULATIONS AND EXPERIMENTAL RESULT:

The proposed transformerless-HSeAF configuration was simulated in MATLAB/Simulink using discrete time steps of

 $Ts = 10 \,\mu s$. A dSPACE/dsp1103 was used for the fast control prototyping. To ensure an error-free and fast implementation, the complete control loop was executed every 40 μs . The

parameters are identified in Table I.

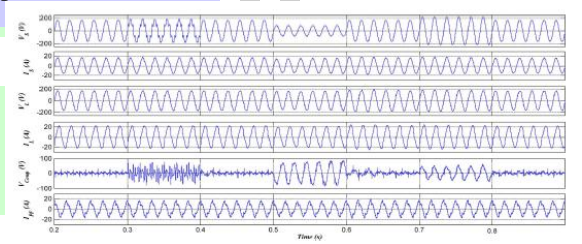


Fig. 11. Simulation of the system with the THSeAF compensating current harmonics and voltage regulation. (a) Source voltage v_S, (b) source current i_S, (c) load voltage v_L, (d) load current i_L, (e) active-filter voltage V_{Comp}, and (f) harmonics current of the passive filter i_{PF}.

The THSeAF reacts instantly to this variation and does not interfere its operation functionality. Meanwhile, it is normal to observe a slight transient voltage variation depending on the

momentum of the load disengagement or connection. To evaluate the compensator during utility perturbation, the power source became distorted as depicted in Fig. 15. The

V. SUMMARY

A DSTATCOM, connected at the point of common coupling (PCC), has been utilized to mitigate both types of PQ problems. When operating in current control mode (CCM), it injects reactive and harmonic components of load currents to make source currents balanced, sinusoidal, and in phase with the PCC voltages. In voltage-control mode (VCM), the DSTATCOM regulates PCC voltage at a reference value to protect critical loads from voltage disturbances, such as sag, swell, and unbalances. However, the advantages of CCM and VCM cannot be achieved simultaneously with one active filter device, since two modes are independent of each other. In CCM operation, the DSTATCOM cannot compensate for voltage disturbances. Hence, CCM operation of DSTATCOM is not useful under voltage disturbances, which is a major disadvantage of this mode of operation . This paper considers the operation of DSTATCOM in VCM and proposes a

control algorithm to obtain the reference load terminal voltage. This algorithm provides the combined advantages of CCM and VCM. The UPF operation at the PCC is achieved at nominal load, whereas fast voltage regulation is provided during voltage disturbances. Also, the reactive and harmonic component of load current is supplied by the compensator at any time of operation. The deadbeat predictive controller is used to generate switching pulses. The control strategy is tested with a three-phase four-wire distribution system. The effectiveness of the IS AS SHOWN IN FGR

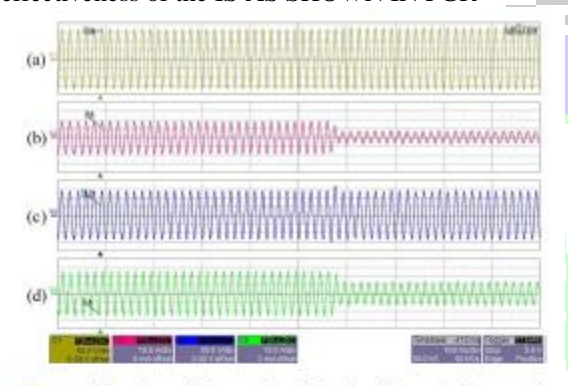


Fig. 14. Waveforms during a dynamic load variation. (a) Source voltage v_E [50 V/div], (b) source current i_E [10 A/div], (c) load PCC voltage v_L [50 V/div], and (d) load current i_L [10 A/div].

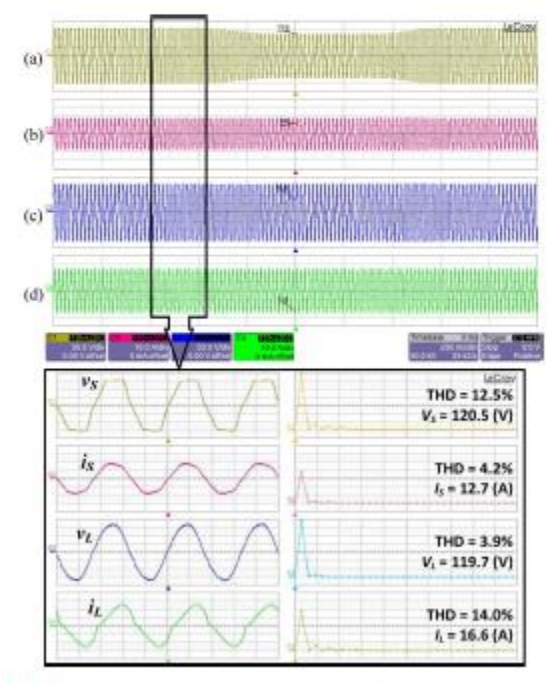


Fig. 15. Experimental waveforms under utility voltage distortion and prolonged sags. (a) Utility source voltage v_S [50 V/div], (b) utility current i_S [10 A/div], (c) load PCC voltage v_L [50 V/div], and (d) load current i_L [10 A/div].

Source of The proposed algorithm is validated through detailed simulation and experimental results. APPENDIX:

For the sake of simplicity, the resistance rc of the switching capacitor filter Cf is neglected, and the inductance Lf has an ideal behavior.

A. Relationship of Load Voltage (V_L) and Grid Voltage (V_S)

$$\begin{split} T_{V_{LS}}(s) &= \frac{V_{L}(s)}{V_{S}(s)} = \frac{Z_{\text{Load}}}{L_{S} + Z_{\text{out}} + Z_{\text{Load}}} = \\ &= \frac{L_{f}L_{L}C_{f}s^{3} + L_{f}R_{L}C_{f}s^{2} + L_{L}s + R_{L}}{A + B + C + D + E + F} \\ A &= L_{f}L_{L}L_{S}C_{f}C_{H}PFs_{5} \\ B &= L_{f}L_{S}R_{L}C_{f}C_{H}PFs^{4} \\ C &= (L_{f}L_{L}C_{f} + L_{f}L_{L}C_{H}PF + L_{f}L_{S}C_{f} \\ &+ L_{L}L_{S}C_{H}PF)s^{3} \\ D &= (L_{f}R_{L}C_{f} + L_{f}R_{L}C_{H}PF + L_{S}R_{L}C_{H}PF)s^{2} \\ E &= (L_{f} + L_{L} + L_{S})s \quad , \quad F &= R_{L}. \end{split}$$

B. Relation Between Load Voltage (V_L) and Compensating Voltage (V_{Comp})

$$\begin{split} T_{V_{CL}}(s) &= \frac{V_{\text{Comp}}}{V_L} = \frac{Z_{\text{out}}}{Z_{\text{Load}}} \\ &= \frac{L_f L_L C_H \, \text{pp s}^{\, 3} + L_f R_L \, C_H \, \text{pp s}^{\, 2} + L_f s}{L_f L_L C_f s^3 + L_f R_L \, C_f s^2 + L_L s + R_L}. \end{split}$$

REFERENCES:

- 1. L. Jun-Young and C. Hyung-Jun, "6.6-kW onboardchargerdesignusingDCMPFCconverterwithh armonic modulation technique and two-stagedc/dc converter," *IEEETrans.Ind.Electron.*, vol.61, no. 3, pp. 1243–1252, Mar. 2014.
- 2. R. Seung-Hee, K. Dong-Hee, K. Min-Jung, K. Jong-Soo, and L. Byoung-Kuk, "Adjustable frequency duty-cycle hybridcontrol strategy for fullbridgeseries resonant converters in electricvehiclechargers," *IEEETrans. Ind. Electron.*, vol. 61,no.10,pp.53545362,Oct. 2014.
- 3. P. T. Staats, W. M. Grady, A. Arapostathis, and R. S.Thallam, "Astatisticalanalysisoftheeffectofelectricv ehiclebatterychargingondistributionsystemharmonicv oltages," *IEEETrans.PowerDel.*, vol. 13, no. 2,pp. 640–646, Apr. 1998.

- 4. A. Kuperman, U. Levy, J. Goren, A. Zafransky, and A. Savernin, "Batterycharger for electric vehicle traction battery switch station," *IEEE Trans.Ind. Electron.*, vol. 60, no. 12, pp. 5391–5399, Dec. 2013.
- 5. Z. Amjadi and S. S. Williamson, "Modeling, simulation, control of anadvanced Luo converter for plug-in hybrid electric vehicle energy-storagesystem," *IEEE Trans. Veh. Technol.*, vol. 60, no. 1,pp. 64–75, Jan. 2011.
- 6. Akagi and K. Isozaki, "A hybrid active filter for a three-phase 12-pulsediode rectifier used as the front end of a medium-voltage motor drive," *IEEE Trans. Power Del.*, vol. 27, no. 1, pp. 69–77, Jan. 2012.
- 7. A. F. Zobaa, "Optimal multiobjective design of hybrid active power filtersconsidering a distorted environment," *IEEE Trans. Ind. Electron.*, vol. 61,no. 1, pp. 107–114, Jan. 2014.
- 9.D. Sixing, L. Jinjun, and L. Jiliang, "Hybrid cascaded H-bridge converterfor harmonic current compensation," *IEEE Trans. Power Electron.*,vol. 28, no. 5, pp. 2170–2179, May 2013.
- 10. S. Hamad, M. I. Masoud, and B. W. Williams, "Medium-voltage12-pulse converter: Output voltage harmonic compensation using a seriesAPF," *IEEE Trans. Ind. Electron.*, vol. 61, no. 1, pp. 43–52, Jan. 2014.
- 11.J. Liu, S. Dai, Q. Chen, and K.Tao, "Modellingand industrial application of series hybridactive power filter," *IETPowerElectron.*, vol. 6, no. 8, pp. 1707–1714, Sep. 2013.

